HHS Public Access

Author manuscript

Nature. Author manuscript; available in PMC 2014 January 04.

Published in final edited form as:

Nature. 2013 July 4; 499(7456): 83–87. doi:10.1038/nature12208.

A single pair of interneurons commands the *Drosophila* feeding motor program

Thomas Flood[1,*], **Shinya Iguchi**[1,*], **Michael Gorczyca**[1,*], **Benjamin White**[2], **Kei Ito**[3], and **Motojiro Yoshihara**[1]

[1]Dept. of Neurobiology, Univ. of Massachusetts Medical School, Worcester, MA.

[2]Laboratory of Molecular Biology, NIMH, Bethesda, MD.

[3]Institute of Molecular and Cellular Biosciences, University of Tokyo, Tokyo, Japan.

Summary

Many feeding behaviors represent stereotyped, organized sequences of motor patterns that have been the subject of neuroethological studies[1,2] such as electrophysiological characterization of neurons governing prey capture in toads[1,3]. Technical limitations, however, have prevented detailed study of the functional role of these neurons as in other studies on vertebrate organisms. Complexities involved in studies of whole animal behavior can be resolved in *Drosophila*, where remote activation of brain cells by genetic means[4] allows one to interrogate the nervous system in freely moving animals to identify neurons that govern a specific behavior, and then to repeatedly target and manipulate these neurons to characterize their function. Here we show finding of neurons that generate the feeding motor program in *Drosophila*. We performed an unbiased screen using remote neuronal activation and identified a critical pair of brain cells that induces the entire feeding sequence when activated. These Fdg (feeding)-neurons are also essential for normal feeding as their suppression or ablation eliminates the sugar-induced feeding behavior. Activation of a single Fdg-neuron induced asymmetric feeding behavior and ablation of a single Fdg-neuron distorted the sugar-induced feeding behavior to be asymmetric, indicating the direct role of these neurons in shaping motor program execution. Simultaneously recording neuronal activity with calcium imaging during feeding behavior[5] further revealed that the Fdg-neurons respond to food presentation, but only in starved flies. Our results demonstrate that Fdg-neurons operate firmly within the sensori-motor watershed, downstream of sensory and metabolic cues and at the top of the feeding motor hierarchy to execute the decision to feed.

Correspondence and requests for materials should be addressed to M.Y. (Motojiro.Yoshihara@umassmed.edu). .
*These authors contributed equally to this work.

Author Information Reprints and permissions information is available at www.nature.com/reprints.

The authors declare no competing financial interests.

Author Contributions M.Y., S.I, T.F., M.G. designed research. T.F. screened Gal4 lines under supervision of K.I and M.Y. T.F., S.I and M.Y. performed behavioral analyses. S.I. performed analyses of ingestion and pump movement, while M.Y. visualized the pump movement. M.G., S.I. K.I. and M.Y. performed neuroanatomy. S.I. and M.Y. did the fly genetics. M.Y. performed calcium imaging. S.I. and M.Y. performed experiments of laser activation and laser ablation with technical assistance of M.G. B.W. contributed TRPM8 and essential advice. M.Y., M.G. and T.F. wrote the paper with assistance from S.I., B.W. and K.I.

Supplementary Information is linked to the online version of the paper at www.nature.com/nature.

To identify neurons controlling feeding behavior we have behaviorally screened flies in which randomly targeted neurons are activated to induce the feeding motor program in a small, temperature-controlled chamber (Supplementary Fig 2). To genetically target random sets of neurons, we took advantage of the collection of "NP lines."[6] Each of these lines expresses the yeast transcription factor Gal4 in a different stereotyped pattern of neurons that depends on the Gal4 insertion site[7]. Gal4-expressing cells were activated by mating flies of each line to flies with a transgene encoding a cold-activated cation channel, TRPM8[8] or a heat-activated-channel, TrpA1[9] under the control of UAS sequences recognized by Gal4. A screen of 835 NP lines identified the Gal4 line NP883, which showed continuous feeding behavior with TrpA1 at elevated temperature. The induced behavior was compared with natural feeding behavior[2] (Fig. 1a-d, Supplementary Fig. 3,4 and Video 1, 2). The natural feeding pattern, evoked by contact with food, is characterized by an initial cessation of locomotion followed by the sequential execution of eight basic motor patterns: (1) all major joints of the fly's forelegs (black arrowheads in Fig. 1a) bend to bring the head closer to the food (dashed horizontal lines for comparison of head heights); (2) the rostrum (magenta arrowheads) projects forward (Fig. 1a-1 to a-3) while (3) the haustellum (blue arrowheads) extends downward (Fig. 1a-1 to a-3), resulting in protrusion of the proboscis; (4) the paired lobes at the tip of the proboscis, called labella (green arrowheads), open upon touching the food to take up food (Fig. 1a-2 to a-3). Taking food, (5) the labella close (Fig. 1a-3 to a-4), and (6) the rostrum and (7) haustellum retract[2,10], returning the entire proboscis to its original position while (8) the forelegs (black arrowheads) raise the body to its original position (Fig. 1a-3 to a-5). The above behavioral sequence was reproduced in a food free environment by TrpA1-mediated activation of neurons in the Gal4-expressing pattern (Fig. 1b and Supplementary Video 2). The TrpA1-induced sequence was well-coordinated, and indistinguishable from natural feeding behavior in the duration of proboscis extension, labellar contact with the substrate, and proboscis retraction (Fig. 1d). We observed repeated labellar opening even with the rostrum and haustellum immobilized (Supplementary Fig. 5, Supplementary Video 2), demonstrating independence of the induced behavioral sequence from sensory cues, which have been thought to be required for labellar lobe opening after contact with food[2,10]. While flies in which the feeding program was induced by TrpA1 stimulation generally opened their labella upon touching the plastic/glass substrate of the chamber (from Fig. 1b-2 to b-3; Supplementary Fig. 3b and 4b), some did so without touching the substrate (Supplementary Fig. 4c,d and Supplementary Video 2). The induced feeding thus represents a "fixed action pattern" [11], which is completely executed without food or substrate, though the natural feeding must be coordinated with sensory stimuli as well. To quantify the feeding behavior induced by stimulation of neurons in the NP883 pattern we adopted the extension and retraction of the rostrum and haustellum (#2, 3, 6, and 7 in the above sequence), referred to as "proboscis extension (PE)." Measured by this index, the induced feeding behavior observed in NP883>*TrpA1* flies at elevated temperature required both the NP883-Gal4 insertion and the TrpA1 transgene (Fig. 1e) and exhibited a temperature-dependence consistent with the activation properties of the dTrpA1 channel (Fig. 1f) in an acute manner in both sexes (Supplementary Fig. 6).

An essential component of feeding behavior not measured by PE is the rhythmic activity of the pharyngeal pump, which is used for swallowing food[2,12,13]. To assess whether the

behavior induced in NP883>*TrpA1* flies includes activation of the pharyngeal pump, we fluorescently labeled the pharyngeal muscles using Myosin heavy chain (Mhc)-GFP[14], (Fig. 2a, b) so that they could be observed through the cuticle. These muscles, m.11, m.12-1 and m.12-2, (Fig. 2b-d) are attached to the upper sclerotized plate out of two sclerotized plates, which lie on top of one another (Fig. 2e, Supplementary Fig. 7a). Observing the action of the pump, using a dye-colored sugar solution to visualize fluid flow upon presentation to a starved fly, revealed the dynamics of pump movement shown in Fig. 2a-e, Supplementary Fig. 7a-c, and Supplementary Video 3. In brief, m.12-1, m.12-2 and m.11 sequentially contract and relax in an alternating manner to lift first the anterior and then the posterior parts of the upper plate to generate rhythmic peristaltic waves of the upper plate which move ingested material from the mouth to the esophagus between the two plates. Counting of individual pump cycles under m.12-1 and m.12-2 (Fig. 2f) revealed that sucrose-induced feeding in a starved fly was mediated by vigorous pumping at 6-8Hz when the temperature was set at 29°C, with the rate declining gradually as the fly became satiated, then leading to a full crop in 2 minutes (Fig. 2g). When we tested NP883>*TrpA1* flies in the Mhc-GFP background, we found that temperature elevation induced intermittent pumping that was indistinguishable from that of natural pumping (Supplementary Video 3). Satiated NP883>*TrpA1* flies showed only occasional pumping at 21°C, but pumped the sugarless dye solution at 6-8Hz at 29 °C in a pattern indistinguishable from that of WT starved flies with sucrose solution (magnified plots in Fig. 2g). Satiated wildtype (WT) flies as controls show much less pumping of the dye solution even at 29 °C than NP883>*TrpA1* flies at 29°C (Fig. 2g), as total pumping pulses were quantified to show 7-fold difference (Supplementary Fig. 7d). Although the induced total pumping during 2 minutes was 40% smaller than the sucrose-induced pumping of starved wildtype flies (Supplementary Fig. 7d), comparison of rates (Fig. 2h) showed that the NP883>*TrpA1* flies continued to pump constantly at the same level as the sucrose-induced pumping of starved wildtype flies after initial vigorous rate. By measuring the net amount of ingested fluid, we observed that in the first 2 minutes, induced pharyngeal pumping led to ingestion of 4.7-fold more fluid than WT controls (Supplementary Fig. 7e), and after approximately 5 minutes led to a full crop although the crop was not filled yet at 2 min (Fig. 2g; Supplementary Video 3). Taken together, our results demonstrate that the activation of Gal4 expressing cells in NP883 produces the complete feeding motor program consisting of all essential motor patterns including pharyngeal pumping.

To identify the specific neurons within the NP883 expression pattern (Fig. 3a, Supplementary Fig. 8a, b, 9) that activate feeding behavior, we used the “flip-out Gal80” technique[15], in which the initially ubiquitous expression of Gal80 is eliminated in small numbers of neurons by the random activation of flippase (see Methods). By this means, we simultaneously expressed TrpA1 and GFP in small subsets of the NP883 pattern and identified the GFP-labeled neurons, whose presence we could correlate with TrpA1-induced feeding. From screening 1,243 flies (Supplementary Fig. 10), we dissected the flies that showed a PE rate of 6 times/min or above, a value not observed in non-flipped out specimens (Supplementary Table 1). Examination of the 40 PE-positive flies led to the identification of one type of interneuron, the GFP expression of which correlated with flies having a higher PE frequency as seen in the histogram of Fig. 3b. We termed this pair of

interneurons “Fdg-neurons”, as shorthand for “feeding neurons”. They possess a distinct and stereotypical morphology with extensive arborization (Fig. 3d, Supplementary Fig. 10c, 11, Supplementary Video 5), which can be unambiguously identified in the full expression pattern of NP883 (arrowheads in Fig. 3a). They are located in the sub(o)esophageal ganglion (SEG/SOG), where axons of gustatory sensory neurons terminate[16-18] (the primary gustatory center, PGC, in the fly brain) and where motoneurons for mouthpart muscles extend their dendritic arbors [10]. To understand information flow to and from the Fdg-neuron, we defined its cellular architecture in relation to these sensory inputs and motor outputs by the “flip-out Gal80” with synaptic markers (Fig. 3e, Supplementary Fig. 12). Fig. 3b shows the distribution of PE rate in the “Fdg-neuron with GFP” group to be significantly skewed to high values in contrast to the “no Fdg-neuron with GFP” group by Mann-Whitney’s U-test. In contrast, another identified neuron type within the NP883 pattern, called ALLH neurons (Supplementary Fig. 13a,b), clearly did not exhibit such a skew (Fig. 3c). In addition, none of the other six prominent SEG cell types within the NP883 expression pattern showed a statistically significant correlation between GFP expression and PE frequency (Supplementary Fig. 13). This was also the case for all cells outside of the SEG (Supplementary Table 2), suggesting that the Fdg-neuron is responsible for the feeding behavior with higher PE rates (see also Supplementary Note 1).

Supplementary Fig. 10d shows the induced behavior (Supplementary Video 4) of the fly, which has strong GFP expression only in a single Fdg-neuron as shown in Fig. 3d and Supplementary Fig. 10c. The behavior induced by TrpA1 in this fly clearly included all eight motor patterns of the natural feeding program following the initial cessation of locomotion, indicating that activation of a single Fdg-neuron can induce the entire sequence of feeding behavior. It should be noted that the feeding behavior observed in Fdg-neuron positive flies contrasted with that of NP883>*TrpA1* flies in that it included more walking (Supplementary Video 4) and lacked leg tremors observed in NP883>*TrpA1* flies (Supplementary Video 2), probably due to removal of activation in other cells. In these respects, the behavior resulting from activation of individual Fdg-neurons more closely mimicked natural feeding behavior. Interestingly, however, we observed an unusual directionality to the PEs produced by flies in which single Fdg-neurons were activated. As shown in Supplementary Fig. 10e, Supplementary Video 4, and Supplementary Table 2, proboscis extension was consistently directed towards the side the GFP-expressing Fdg-neuron was on. This asymmetric regulation of proboscis extension by the Fdg-neuron suggests that each Fdg-neuron may selectively regulate the strength of proboscis muscle contraction on the same side of the body, consistent with the observation that presentation of food to gustatory receptors on one side of the body leads to proboscis extension on that side (Supplementary Video 1).

To determine whether Fdg-neuron activity is required for natural feeding, we first suppressed activity of all neurons in the NP883-Gal4 pattern, by the expression of an inward rectifier potassium channel, Kir[19], leading to abolishment of natural feeding behavior in response to sucrose (Supplementary Fig. 14, Supplementary Video 6). The major sugar sensing neurons of the labellum, which express the gustatory receptor Gr5a[16,17], terminate in the vicinity of Fdg-neuron’s dendrite, but careful confocal analysis revealed no direct

contact between the processes of the two types of neurons (Supplementary Fig. 15). To determine whether the Fdg-neurons receive indirect input from the sugar-sensing neurons, we assayed their response to gustatory stimuli by calcium imaging using a genetically encoded Ca^{2+} indicator, GCaMP3.0[20], driven by NP883-Gal4. To achieve this, we used a specially designed setup (i.e. the Feeding circuit/Fly brain Live Imaging and Electrophysiology Stage, or FLIES) to visualize SEG neurons through an opening in the head[5] (Fig. 4a,b). As shown in Fig. 4c, stimulation of the labellar lobes of a starved fly with 400 mM sucrose, resulted in brief lobe opening, and a simultaneous, large increase in GCaMP3.0 fluorescence in the cell body of the Fdg-neuron (Supplementary Video 7). This response was specific insofar as adjacent neurons, called LPEs (Supplementary Fig. 13, 16a), showed no increase in GCaMP3.0 fluorescence even in starved flies (Supplementary Fig. 17a). Furthermore, RFP fluorescence did not change with the sucrose stimulus (Fig. 4c, Supplementary Fig. 17a). Interestingly, neither labellar opening nor Ca^{2+} elevation in the Fdg-neuron was observed in satiated flies (Supplementary Fig. 17). Our results thus indicate that sucrose acutely activates the Fdg-neurons, and that this response is contingent on the metabolic state of the animal.

The FLIES setup allowed us to image and focally heat the cell body of a single Fdg-neuron expressing TrpA1 and GFP using limited illumination of the infrared (IR) laser of a two-photon microscope for activation of Fdg-neuron (see Method, Supplementary Fig. 16b). As expected from the results of our “flip-out Gal80” studies, this stimulus caused immediate asymmetric PE to the side of the stimulated neuron (Fig. 4d, Supplementary Video 8). It also induced pump movement (Fig. 4d, Supplementary Video 8). In contrast, selective illumination of an LPE neuron, located only 10-20 μm from the Fdg-neuron (Supplementary Fig. 13, 16a, c), failed to induce PE or pump movement at the same stimulus level (see Method, Supplementary Video 8). These results directly confirmed that activation of Fdg-neuron can trigger feeding behavior in a specific manner.

To test the requirement for the Fdg-neuron in natural feeding behavior, we selectively ablated Fdg-neurons in starved NP883>*GFP* flies using stronger laser illumination (see Method, Supplementary Fig. 16d). Ablation of the Fdg-neuron on one side, followed by stimulation with 400 mM sucrose triggered PE in the direction opposite to the ablated side, while ablation of the Fdg-neurons on both sides completely eliminated the response to sucrose (Fig. 4e, Supplementary Video 9). In control experiments, ablation of the nearby LPE neuron did not affect the PE response, again demonstrating the specificity of the manipulation. Consistent with the results of Kir suppression (Supplementary Fig. 14), these results demonstrate that Fdg-neurons are essential for natural feeding in the fly and demonstrate the absence of neurons with redundant function.

The induction of the entire feeding program by Fdg-neuron activation contrasts with the effects of activating motor neurons that innervate muscles of the proboscis[21] or the pharyngeal pump[22]. The induction of feeding by Fdg-neurons is likewise distinct from that produced by stimulation of AgRP/NPY-expressing neurons in the mammalian hypothalamus, which has long latencies (i.e. minutes vs. seconds) and involves indirect regulation of motor output[23]. Their activity encodes metabolically-derived motivational cues and contrasts with that of the Fdg-neurons which clearly encodes integrated information of

both gustatory and metabolic origin, and drives motor output in a manner that is perhaps most reminiscent of the "command neurons" first described by Wiersma and Ikeda in the crayfish[24]. The motor—as opposed to motivational—function of the Fdg-neurons is evident in their asymmetric control of proboscis extension, which indicates a specific role of each Fdg-neuron in contraction of a subset of the proboscis musculature. How the Fdg-neurons coordinate the various motor patterns involved in feeding remains to be determined. Pump rhythms (Fig. 2), like the well-characterized movements of the crustacean stomatogastric nervous system, may result from the action of a central pattern generator (CPG) governed by intrinsic membrane properties and inhibitory interactions of the component neurons[25]. Recently, co-activation of motoneurons controlling m.11 and m.12-1 has been shown to generate rhythmic contractions of the pharyngeal pump[22], and activation of these neurons by the Fdg-neurons might be the source of the pump CPG[2]. As seen in Supplementary Video 5, the large dendritic arbor of the Fdg-neuron, which is reminiscent of the putative feeding neurons of toads[1,3] and courtship neurons of *Drosophila*[26], suggest a role in integrating information beyond sugar and starvation cues, including perhaps other gustatory cues, such as bitter or salty, and signals of other modalities. In any case, our laser ablation experiments suggest that inputs that govern feeding responses likely pass through the single pair of Fdg-neurons. The identification of these neurons here and the demonstration of their pivotal position in the feeding circuit open the door to systematic future experiments on their roles in sensory integration and its plasticity in fly feeding behavior.

Methods

Fly strains

Drosophila crosses were performed at 21°C or 25°C according to standard protocols. Canton S was used as the wildtype control. Transgenic strains were balanced with *FM7c*, *CyO*, *TM3*, or *TM6B* chromosomes. *UAS-TRPM8* has been previously described[8]. *UAS-TrpA1*[9] was obtained from P. Garrity. *UAS-mCD8-mCherry* was made by A. Sheehan, and generously provided by M. Freeman before publication. *Myosin Heavy Chain* (*Mhc*)*-GFP* was from K. Gajewski[14], *UAS-mCD8-GFP*[30] and a heat-shock-flippase (*HS-FLP*) strain[15] were from T. Lee. *>Tubulin-Gal 80>*, made by G. Struhl, was from M. Roshbash[31], *elav-Gal80* [32] was from Y.-N. Jan, *Mhc-Gal80*[33] was from L. Luo, *Choline-acetyl transferase-Gal80*[34] was from S. Waddell, *UAS-BRP-GFP*[35] and *UAS-nAChR-GFP* (*UAS-Dα7-GFP*)[36] were from S. Sigrist, *UAS-n-synaptobrevin-GFP*[37] was from M. Ramaswami, *Gr5a-GFP-IRES-GFP-IRES-GFP*[38] was from K. Scott, *UAS-Kir2.1*[39] was from V. Budnik, *tubP-Gal80*^{ts} [40] was from S.Waddell. *UAS-GCaMP3.0*[20] was from L. Looger, and *UAS-mCD8-RFP* was from T. Awasaki[41] .

We used two Gal4 strains that were established by the NP consortium[6]. The NP883 line has a Gal4 insertion approximately 500 base pairs 5′ upstream of the UTR of *Cyp6a14*[42], a locus encoding a member of the cytochrome P450 family, which functions for electron transfer. Although none of the Gal4 lines screened showed temperature-induced behavior similar to NP883, another NP line not included in the screen, NP5137 was later identified as having an insertion at a more proximal site to the coding region of *Cyp6a14*[42]. This line exhibited a

similar pattern of feeding behavior (Fig. 1e,f) when driving TrpA1, and included Fdg-neuron in its expression pattern common to NP883 (Supplementary Fig. 8c).

Observation of fly behavior

For observing TrpA1-induced behavior, we used a custom built plastic chamber (Supplementary Fig. 2), which enabled the temperature gradient to be maintained within ± 1 °C from its floor to ceiling (height 4 mm) at experimental temperatures. The chamber was designed to fit snuggly into a Nunc 35 mm plastic dish, and temperature was regulated by a TS-4 SPD Controller (Physitemp) and monitored with an IT-23 probe connected to a microprobe thermometer, BAT-10 (Physitemp) (Supplementary Fig. 2). The inside of the fly chamber was cleaned after each use. We observed fly behavior by usual techniques (see Supplementary Methods).

For observing labellar movement with immobilized proboscis (Supplementary Fig. 5), we anesthetized a fly in a 15 ml plastic tube immersed in ice, and placed the fly in a Pipetman tip with its tip cut to expose its head[43]. The rostrum and haustellum of the fly's proboscis were fixed using light-curing glue (Tetric EvoFlow, Ivoclar Vivadent). The fly held in the Pipetman tip was videotaped for 1 minute at 21°C. Then, the Pipetman tip holding the fly was placed in the temperature-controlled chamber prewarmed to 31°C -32°C. 1 minute later, when the temperature monitored by the temperature probe reached 31°C-32°C, we videotaped the labellar lobes for 1 minute. After that, we took the Pipetman tip holding the fly out from the chamber and placed it in the room at 21°C, and we videotaped labellar lobes for 1 minute.

Visualization and quantification of pump movement and quantification of dye ingestion amount

For visualization of pump movement, a fly with *Myosin heavy chain* (*Mhc*)-*GFP*[14] was constrained in a Pipetman tip as stated above. For natural feeding, an aqueous 100 mM sucrose solution with 0.03mg/ml Brilliant Blue FCF (Acros Organics) was provided to a 24 hours starved fly through a hypodermic needle. For visualizing m.11, the hypodermic needle was placed anterior to make the rostrum fully protracted. For induced feeding, the rostrum of a fly with NP883>*TrpA1* with *Mhc-GFP* constrained in a Pipetman tip was glued to be immobilized at fully protracted position with light curing glue. Then, the Pipetman was placed in the temperature-controlled chamber with small holes, through which a hypodermic needle passed to provide the blue dye solution. The hypodermic needle was loaded on a joystick manipulator (Narishige, MN-151) and connected with a flexible plastic tube to an injector (Narishige, IM-5B) to constantly supply dye solution. Fluorescence from Mhc-GFP was observed using Leica MZ10F with a CCD camera for videotaping. This fluorescence was supplemented with additional light from fiber optics to visualize the fly's mouthpart structures. We noticed that in partially satiated WT flies and sometimes in NP883>*TrpA1* flies, contractions of m.12-1 and m.12-2 were not necessarily associated with those of m.11 (Supplementary Video 3), causing backward flow from the spherical lumen[22] (Supplementary Video 3). To directly quantify ingestion, we therefore measured the net amount of ingested fluid as follows.

For quantification of pump movement and ingestion amount, a tethered fly at its back was provided with the dye solution through a glass capillary tube, which was loaded on a manipulator and connected to a manipulator as stated above. The glass capillary allowed us to measure the amount of solution ingested by measuring the length of dye solution filling the capillary. In the same experiments, the fly was videotaped with a CCD camera through a Nikon SMZ-800, and dye movement under m.12-1 and m.12-2 (Fig. 2f) was characterized.

Immunohistochemistry

We performed immunostaining according to a protocol described previously[27] with a modification for adult brains (see Supplementary Methods for details).

Flipping screening for feeding flies

We used flies with the following genotype for flipping experiments for TrpA1 and GFP;

HS-FLP (X-chromosome) ; >*Tubulin-Gal80*> *UAS-TrpA1*/ NP883 (2nd Chromosomes); *UAS-mCD8-GFP*/+ (3rd Chromosomes).

We used flies with the following genotype for flipping experiments for TrpA1, mCherry and BRP-GFP;

HS-FLP (X-chromosome) ; >*Tubulin-Gal80*> *UAS-TrpA1*/ NP883 (2nd Chromosomes); *UAS- mCD8-mCherry UAS-BRP-GFP* / + (3rd Chromosomes).

A series of similar experiments was also performed using *UAS-n-synaptobrevin-GFP*[37] instead of *UAS-BRP-GFP*.

We used flies with the following genotype for flipping experiments for TrpA1, mCherry and nAChR-GFP;

HS-FLP (X-chromosome) ; >*Tubulin-Gal80*> *UAS-TrpA1*/ NP883 (2nd Chromosomes); *UAS-mCD8-mCherry UAS-nAChR-GFP* / + (3rd Chromosomes).

We used flies with the following genotype for flipping experiments for TrpA1, mCherry and Gr5a-GFP;

Gr5a-GFP-IRES-GFP-IRES-GFP / *HS-FLP* (X-chromosome) ; >*Tubulin-Gal80*> *UAS-TrpA1*/ NP883 (2nd Chromosomes); *UAS-mCD8-mCherry* / + (3rd Chromosomes).

These flies were aged for 2-5 days after eclosion, and tested at 37°C to observe feeding behavior. Behavior was quantified by counting PEs for 1min after an incubation period of 30 seconds upon introduction into the behavioral chamber. Heat shock was not necessary as flipping was active at normal temperature (21°C). For assessing asymmetry, we analyzed movie frames with bottom views, and judged asymmetry if the center of labella extended beyond 5% of the distance between the midline and lateral edge of the fly's head at least 3 times.

For describing Fdg-neuron branching pattern, more than ten samples with an isolated and complete Fdg-neuron were analyzed in detail from the behavioral screening described in the text. For each analysis of cellular architecture, at least four good samples for each genotype were analyzed in detail by isolating, staining and microscoping more than ten feeding-positive flies from each series of behavioral screening.

Suppression by Kir2.1 channel

The inward rectifier potassium channel[19,44], Kir2.1[39] was expressed exclusively in the adult stage using the TARGET system[40] to avoid any developmental effects. Flies with NP883, *UAS-Kir2.1*, *tubP-Gal80^{ts}* were reared at 19°C, and collected within one day after eclosion. NP883, *UAS-Kir2.1* flies were lethal, thus, the suppression by Gal80^{ts} through development was mandatory. The flies were starved and temperature-shifted in the protocols depicted in Supplementary Fig. 14. They were starved in a vial with a wet paper towel at the bottom. Starved flies were anesthetized by chilling in a test tube standing on ice, and gently held by Pipetman tip as previously described[43]. For observation of proboscis extension response (PER), the proboscis was stimulated by a 100 mM aqueous sucrose solution on a wick inserted into a 1ml syringe[5]. A special ultrathin and smooth, traditional Japanese Washi paper (Haibara, Japan) was used as a wick. This was sturdy and held solution well and was transparent when wet, all improvements for reducing experimental variation when compared to KimWipes[43]. After making a very small droplet of sugar solution at the wick, the piston of the syringe was pulled, and at the moment when the droplet was sucked, the wet surface of the Washi wick was applied to the tip of proboscis. These manipulations were done quickly to prevent the animal from drinking sucrose solution and mitigating its starved state (Supplementary Video 6). Before sucrose application water was applied to make sure the fly was not thirsty. If the fly responded just to water, it was given water to the point of satiation. Each fly was given 5 presentations of sucrose solution and PER was counted. Between each sucrose presentation water was applied to clean labellar lobes. Since no difference between males and female was recognized, half of the results were from male flies and half were from females.

For observation of free running behavior with Kir2.1, flies of certain genotype were placed individually in a chamber (3.5 mm × 10 mm, 2mm height) with a sheet (1 mm thickness) of standard fly food on one side (10 mm × 2 mm). Behavior was observed for 2 minutes and videotaped in the 2.5 mm × 10 mm (2 mm height) space through the top glass (3.5 mm × 10 mm) at each time point for each genotype. Proboscis extension (PE) that reached the food was counted for 30 second, 1 min-1.5min after placing the fly into the chamber, and PE per minutes was calculated.

Calcium imaging with observation of proboscis extension response

Ca^{2+} imaging as well as laser activation and ablation were performed using the Feeding circuit/ Fly brain Live Imaging and Electrophysiology Stage (FLIES), which was designed to expose the brain of a fly for general purposes such as live imaging, electrophysiology and to keep the fly's proboscis dry and free for movement[5]. Ca^{2+} imaging was performed by a method modified from that previously reported[5]. An adult fly was anesthetized in a 15 ml plastic tube standing on ice and set in a tube attached to a FLIES apparatus. Light-curing

glue was used to seal the proximally adjacent part of the rostrum to the inner edge of the chamber's hole. To minimize movement artifact, we immobilized the proboscis, which we kept half extended to prevent the pump unit from bumping into and from occluding the SEG, with light curing glue leaving only labellar lobes free to move. A sugar-free saline used previously for *Drosophila* embryonic electrophysiology was also employed here[28]. The saline contained (in mM): NaCl, 140; KCl, 2; $MgCl_2$, 4.5; $CaCl_2$, 1.5; and HEPES-NaOH, 5, pH 7.1. The head capsule was opened by a tungsten "sword", which was originally designed for dissection of a *Drosophila* embryo[29], and by "scisceps" which are forceps modified to act as scissors to better clip the cuticle and trachea and expose the SEG. The esophagus, Muscle 16[12] and the antennal nerves were removed, and air sacks were stretched to the side to expose an Fdg-neuron's cell body and to avoid movements that could add noise to the Ca^{2+} signal. Ca^{2+} imaging was performed following a previous report[45]. We scanned the cell body of an Fdg-neuron through a 40X water immersion lens (0.80 n.a.), using the spinning disk confocal laser system, CSU X1 (Improvision Inc./Yokogawa Inc.) using Velocity software, ver. 4.3, on a BX51WI microscope (Olympus). mCD8-RFP was co-expressed to check movement artifact, and GCaMP3.0 and mCD8-RFP were labeled at the same time. GCaMP3.0 signal was imaged with an exposure time of 300 ms of 491nm laser for detection, and mCD8-RFP fluorescence was imaged with a 535 nm laser with an exposure time of 100 ms every 1.4 sec. GCaMP3.0 fluorescence and mCD8-RFP fluorescence at the cell body of an Fdg-neuron were quantified at a region of interest using the Volocity software (Improvision). Identification of an Fdg-neuron by its location was confirmed by immunostaining with anti-GFP antibody recognizing GCaMP 3.0 after Ca^{2+} imaging experiments. Throughout the experiments, saline was slowly (one drop/second) perfused. Perfusion dramatically reduced the spontaneous movement of a proboscis, which is one major source of movement artifact. The proboscis was stimulated by an aqueous sucrose solution in the same manner as PER experiments with Kir suppression. Labellar bristles (Supplementary Fig. 3a) sensed the sucrose and the proboscis extended reproducibly if flies were starved for 24 hours immediately before PER experiments (Supplementary Video 7). Proboscis extension response (PER) behavior was monitored and recorded through a CCD camera attached to a dissection microscope (SMZ-800, Nikon) supported by a swing arm at the same time as GCaMP3.0 was being imaged by the spinning disk confocal microscope[5]. In the case of NP883> *GCaMP3.0* flies, starvation effect is accelerated probably due to interaction between GCaMP3.0 and cellular Ca^{2+} ions, and these flies show a full PER in response to 100 mM sucrose by only 13 hours of starvation. Starvation for too long, such as 24 hours, decreases the probability of PER. Therefore, we started dissection in this series of Ca^{2+} imaging experiments at around 13 hours of starvation. To gain an unambiguous response, we stimulated with 400 mM sucrose because weak responses by 100 mM sucrose tended to be confused with background activity or movement artifact even after several attempts to reduce movement artifact as stated above. We checked PER by 100 mM sucrose before dissection, and only flies exhibiting PER behavior were dissected. For satiated experiments, flies were placed in a grape juice/yeast pasted food vial for more than 1 hour, and only flies that did not show a PER to sucrose stimulation were dissected. We took data within one and a half hour after starting dissection. Details of these methods were published[5], but many details were improved from the published methods to minimize movement artifact to unambiguously detect small responses in Fdg-neurons.

Laser activation and laser ablation of an Fdg-neuron

The FLIES apparatus was used, and experiments were performed under the Zeiss two-photon microscope, LSM 7 MP. The fly was set into the FLIES apparatus stated above, but the proboscis was left free for observation of its movement, especially for testing asymmetry of PE. Dissection was done in the same manner as in the Ca^{2+} imaging experiments. We used the same saline as that used for Ca^{2+} imaging in this series of laser activation and ablation experiments.

For laser activation, we first briefly imaged a satiated NP883>*TrpA1; mCD8-GFP* fly and identified an Fdg-neuron and LPE neuron (control), limiting infrared (IR) illumination as much as possible to avoid triggering activity (Supplementary Fig. 16). Then we set a 15.4 μm (55 pixel at 3 X-zoomed condition, pixel size=0.28 μm) diameter region of interest (ROI) surrounding the cell body (Fdg-neuron or LPE neuron). We set the circle at a diameter, which was twice the diameter of the cell, so as not to miss the cell body even after small movements, which were inevitable because the proboscis was moving freely. Using the "test bleaching" program of the LSM 7 MP system's Zen software, we scanned the area of the circle for 120 msec total (4 iterations) with 20% power at a laser setting of 870 nm. We set the scan speed at 5, which corresponded to a pixel dwell time of 12.61 μsec, and selected the "zoom bleach" function on the software. This scanning protocol was repeated 3 times approximately 10 seconds apart. We could see an obvious PE usually by the 3rd scanning but sometimes earlier, presumably by a facilitative effect. Only one neuron was illuminated for each preparation either for Fdg-neuron or LPE neuron to exclude the possibility of activating the cell as a result of repeated laser scanning. At the end of the experiment, a live scan of the cell body was taken, and no obvious damage was observed (Supplementary Fig. 16b, c). We positioned a Nikon SMZ-800 stereomicroscope supported with a swing arm in front of the fly to observe and videotape movement of the proboscis, using fiber illumination. To suppress background TrpA1 opening and to improve the spacio-temporal resolution of laser activation, we perfused saline chilled to 21°C during the entire experiment.

For laser activation observing pump movement, a similar experimental set-up was used as described above, except the esophagus was left intact to allow proper ingestion of dye aqueous solution. The rostrum of the proboscis was extended out with gentle vacuum and glued to the eaves of the FLIES apparatus with light curing glue to visualize the pharyngeal pump. Prior to activation, flies were allowed access to ingest dye solution for avoiding dehydration. Numbers of samples were; 4 (Fdg-neuron for PE), 5 (Fdg-neuron for pumping), 5 (LPE neuron for PE), 5 (LPE neuron for pumping). All preparation for the Fdg-neuron showed positive effects, that is, PE in the direction to the same side as illuminated Fdg-neuron, or a pump pulse just after laser illumination on either side of Fdg-neuron. Control illumination on LPE-neuron had no obvious effect on PE or pump pulses. In the absence of TrpA1 expression, we saw no induction of feeding behavior upon IR illumination of the Fdg-neuron, also confirming the specificity of the manipulation (data not shown, n=5).

For laser ablation, we used basically the same type of experimental set up as that for laser activation. We first briefly imaged a starved NP883> *mCD8-GFP* fly and identified an Fdg-

neuron and an LPE neuron. Then we set 2.8 μm (10 pixel at 3 X-zoomed condition, pixel size= 0.28μm) diameter circle inside the targeted cell body (Fdg-neuron or LPE neuron). We set the scan speed at 4, which corresponded to a pixel dwell time of 25.21 μsec, and selected the "zoom bleach" function within the software. Using the "test bleaching" program, we scanned the area of the circle for 10 msec as total (5 iterations) with 30% power at 870 nm. The strong laser made a damaged looking cell body (arrowhead in Supplementary Figure 16d) to confirm that the cell was ablated. In some cases, we could observe a small transient bubble, which shrank and disappeared in a few seconds, then end up with the aforementioned damaged look. Before and after ablation, we tested PER with 400 mM sucrose stimulation. We perfused saline chilled to 21°C during all experiments. After ablation of a neuron, we waited for 15 minutes until ablation effect appeared on PER. Numbers of samples were; 5 (Fdg-neuron), 5 (LPE neuron). All Fdg-neuron ablation gave consistent results with Fig. 4e and Supplementary Video 9 while ablation of LPE-neuron showed no recognizable effect on PE.

For assessing asymmetry both in laser activation and in laser ablation, we analyzed movie frames, and judged asymmetry if the midline of the labella extended beyond 5% of the distance between the midline and the lateral edge of the fly's head.

Statistics

All statistic analyses were performed according to standard methods[46] using Prism, ver. 5.0a (GraphPad Software, Inc.) and Excel (Microsoft).

For statistics in Fig. 1e, the six groups were analyzed with the Kruskal-Wallis test using a one-way ANOVA by ranks, and the significant difference between groups was found ($P<0.0001$). Triple asterisks (***) denote $P<0.001$ by Dunn's post-hoc multiple comparison test between progeny from this cross: NP883 × *UAS-TrpA1* (NP883>*TrpA1*), compared to these crosses NP883 × WT, WT × *UAS-TrpA1*, or WT × WT. The same post-hoc analysis was performed for the NP5137 line.

Supplementary Material

Refer to Web version on PubMed Central for supplementary material.

Acknowledgements

We thank S. Waddell for critical discussion, fly stocks and reading of the manuscript; T. Lee for critical discussion and fly stocks; A. Sakurai for critical reading of the manuscript; S. Reppert for support; M. Alkema and T. Ip for discussions; members of the NP consortium for NP lines; T. Awasaki., C. Kao, V. Budnik, P. Garrity, M. Freeman, M. Rosbash, Y.-N. Jan, L. Luo, S. Sigrist, K. Scott, T. Tanimura, L. Looger, M. Ramaswami, K. Gajewski for fly stocks; K. Ikeda, T. Tanimura and H. Ishimoto for technical advices; A.Taylor and R. Seeham for technical help; Nobuko Yoshihara for material information. This work was supported by National Institute of Mental Health Grants MH85958, and the Worcester Foundation (to M.Y.), and the summer program of the Japan Society for the Promotion of Science/National Science Foundation (to T.F), and a Japan Science and Technology Agency CREST grant (to K.I.).

References

1. Ewert JP. Neural correlates of key stimulus and releasing mechanism: a case study and two concepts. Trends Neurosci. 1997; 20(8):332–339. [PubMed: 9246720]

2. Dethier, VG. Hungry Fly. Harvard University Press; 1976.
3. Matsushima T, Satou M, Ueda K. Medullary reticular neurons in the Japanese toad: morphologies and excitatory inputs from the optic tectum. J Comp Physiol A. 1989; 166(1):7–22. [PubMed: 2600886]
4. Lima SQ, Miesenbock G. Remote control of behavior through genetically targeted photostimulation of neurons. Cell. 2005; 121(1):141–152. [PubMed: 15820685]
5. Yoshihara M. Simultaneous recording of calcium signals from identified neurons and feeding behavior of *Drosophila melanogaster*. J Vis Exp. 2012; 62:w3625.
6. Yoshihara M, Ito K. Improved Gal4 screening kit for large-scale generation of enhancer-trap strains. Dros. Inf. Serv. 2000; 83:199–202.
7. O'Kane CJ, Gehring WJ. Detection in situ of genomic regulatory elements in *Drosophila*. Proc Natl Acad Sci U S A. 1987; 84(24):9123–9127. [PubMed: 2827169]
8. Peabody NC, et al. Characterization of the decision network for wing expansion in *Drosophila* using targeted expression of the TRPM8 channel. J Neurosci. 2009; 29(11):3343–3353. [PubMed: 19295141]
9. Hamada FN, et al. An internal thermal sensor controlling temperature preference in *Drosophila*. Nature. 2008; 454(7201):217–220. [PubMed: 18548007]
10. Singh RN. Neurobiology of the gustatory systems of *Drosophila* and some terrestrial insects. Microsc Res Tech. 1997; 39(6):547–563. [PubMed: 9438253]
11. Tinbergen, N. The study of Instinct. Clarendon Press; Oxford: 1989.
12. Miller, A. The internal anatomy and histology of the imago of *Drosophila melanogaster*. In: Demerec, M., editor. Biology of Drosophila. John Wiley & Sons; 1950. p. 420-534.
13. Ferris, GF. External morphology of the adult. In: Demerec, M., editor. Biology of Drosophila. John Wiley & Sons; 1950. p. 368-419.
14. Gajewski KM, Schulz RA. CF2 represses Actin 88F gene expression and maintains filament balance during indirect flight muscle development in *Drosophila*. PLoS One. 2010; 5(5):e10713. [PubMed: 20520827]
15. Struhl G, Basler K. Organizing activity of wingless protein in *Drosophila*. Cell. 1993; 72(4):527–540. [PubMed: 8440019]
16. Wang Z, Singhvi A, Kong P, Scott K. Taste representations in the *Drosophila* brain. Cell. 2004; 117(7):981–991. [PubMed: 15210117]
17. Thorne N, Chromey C, Bray S, Amrein H. Taste perception and coding in *Drosophila*. Curr Biol. 2004; 14(12):1065–1079. [PubMed: 15202999]
18. Miyazaki T, Ito K. Neural architecture of the primary gustatory center of *Drosophila* melanogaster visualized with GAL4 and LexA enhancer-trap systems. J Comp Neurol. 2010; 518(20):4147–4181. [PubMed: 20878781]
19. Hagiwara S, Miyazaki S, Moody W, Patlak J. Blocking effects of barium and hydrogen ions on the potassium current during anomalous rectification in the starfish egg. J Physiol. 1978; 279:167–185. [PubMed: 566793]
20. Tian L, et al. Imaging neural activity in worms, flies and mice with improved GCaMP calcium indicators. Nat Methods. 2009; 6(12):875–881. [PubMed: 19898485]
21. Gordon MD, Scott K. Motor control in a *Drosophila* taste circuit. Neuron. 2009; 61(3):373–384. [PubMed: 19217375]
22. Manzo A, Silies M, Gohl DM, Scott K. Motor neurons controlling fluid ingestion in *Drosophila*. Proc Natl Acad Sci U S A. 2012; 109(16):6307–6312. [PubMed: 22474379]
23. Aponte Y, Atasoy D, Sternson SM. AGRP neurons are sufficient to orchestrate feeding behavior rapidly and without training. Nat Neurosci. 2011; 14(3):351–355. [PubMed: 21209617]
24. Wiersma CA, Ikeda K. Interneurons Commanding Swimmeret Movements in the Crayfish, Procambarus Clarki (Girard). Comp Biochem Physiol. 1964; 12:509–525. [PubMed: 14206963]
25. Marder E, Bucher D. Understanding circuit dynamics using the stomatogastric nervous system of lobsters and crabs. Annu Rev Physiol. 2007; 69:291–316. [PubMed: 17009928]

26. Kimura K, Hachiya T, Koganezawa M, Tazawa T, Yamamoto D. Fruitless and doublesex coordinate to generate male-specific neurons that can initiate courtship. Neuron. 2008; 59(5):759–769. [PubMed: 18786359]
27. Yoshihara M, Rheuben MB, Kidokoro Y. Transition from growth cone to functional motor nerve terminal in *Drosophila* embryos. J Neurosci. 1997; 17(21):8408–8426. [PubMed: 9334414]
28. Yoshihara M, et al. Selective effects of neuronal-synaptobrevin mutations on transmitter release evoked by sustained versus transient Ca^{2+} increases and by cAMP. J Neurosci. 1999; 19(7):2432–2441. [PubMed: 10087058]
29. Yoshihara M, Adolfsen B, Galle KT, Littleton JT. Retrograde signaling by Syt 4 induces presynaptic release and synapse-specific growth. Science. 2005; 310(5749):858–863. [PubMed: 16272123]
30. Lee T, Luo L. Mosaic analysis with a repressible cell marker for studies of gene function in neuronal morphogenesis. Neuron. 1999; 22(3):451–461. [PubMed: 10197526]
31. Shang Y, Griffith LC, Rosbash M. Light-arousal and circadian photoreception circuits intersect at the large PDF cells of the *Drosophila* brain. Proc Natl Acad Sci U S A. 2008; 105(50):19587–19594. [PubMed: 19060186]
32. Yang CH, et al. Control of the postmating behavioral switch in *Drosophila* females by internal sensory neurons. Neuron. 2009; 61(4):519–526. [PubMed: 19249273]
33. Pauli A, et al. Cell-type-specific TEV protease cleavage reveals cohesin functions in *Drosophila* neurons. Dev Cell. 2008; 14(2):239–251. [PubMed: 18267092]
34. Kitamoto T. Conditional disruption of synaptic transmission induces male-male courtship behavior in *Drosophila*. Proc Natl Acad Sci U S A. 2002; 99(20):13232–13237. [PubMed: 12239352]
35. Fouquet W, et al. Maturation of active zone assembly by *Drosophila* Bruchpilot. J Cell Biol. 2009; 186(1):129–145. [PubMed: 19596851]
36. Leiss F, et al. Characterization of dendritic spines in the *Drosophila* central nervous system. Dev Neurobiol. 2009; 69(4):221–234. [PubMed: 19160442]
37. Estes PS, Ho GL, Narayanan R, Ramaswami M. Synaptic localization and restricted diffusion of a *Drosophila* neuronal synaptobrevin--green fluorescent protein chimera in vivo. J Neurogenet. 2000; 13(4):233–255. [PubMed: 10858822]
38. Fischler W, Kong P, Marella S, Scott K. The detection of carbonation by the *Drosophila* gustatory system. Nature. 2007; 448(7157):1054–1057. [PubMed: 17728758]
39. Baines RA, Uhler JP, Thompson A, Sweeney ST, Bate M. Altered electrical properties in *Drosophila* neurons developing without synaptic transmission. J Neurosci. 2001; 21(5):1523–1531. [PubMed: 11222642]
40. McGuire SE, Le PT, Osborn AJ, Matsumoto K, Davis RL. Spatiotemporal rescue of memory dysfunction in *Drosophila*. Science. 2003; 302(5651):1765–1768. [PubMed: 14657498]
41. Awasaki T, Lai SL, Ito K, Lee T. Organization and postembryonic development of glial cells in the adult central brain of *Drosophila*. J Neurosci. 2008; 28(51):13742–13753. [PubMed: 19091965]
42. Hayashi S, et al. GETDB, a database compiling expression patterns and molecular locations of a collection of Gal4 enhancer traps. Genesis. 2002; 34(1-2):58–61. [PubMed: 12324948]
43. Shiraiwa T, Carlson JR. Proboscis extension response (PER) assay in *Drosophila*. J Vis Exp. 2007; 193(3)
44. Kubo Y, Baldwin TJ, Jan YN, Jan LY. Primary structure and functional expression of a mouse inward rectifier potassium channel. Nature. 1993; 362(6416):127–133. [PubMed: 7680768]
45. Marella S, et al. Imaging taste responses in the fly brain reveals a functional map of taste category and behavior. Neuron. 2006; 49(2):285–295. [PubMed: 16423701]
46. Zar, J. Biostatistical Analysis. 4th ed. Prentice Hall; Upper Saddle River, NJ: 1999.

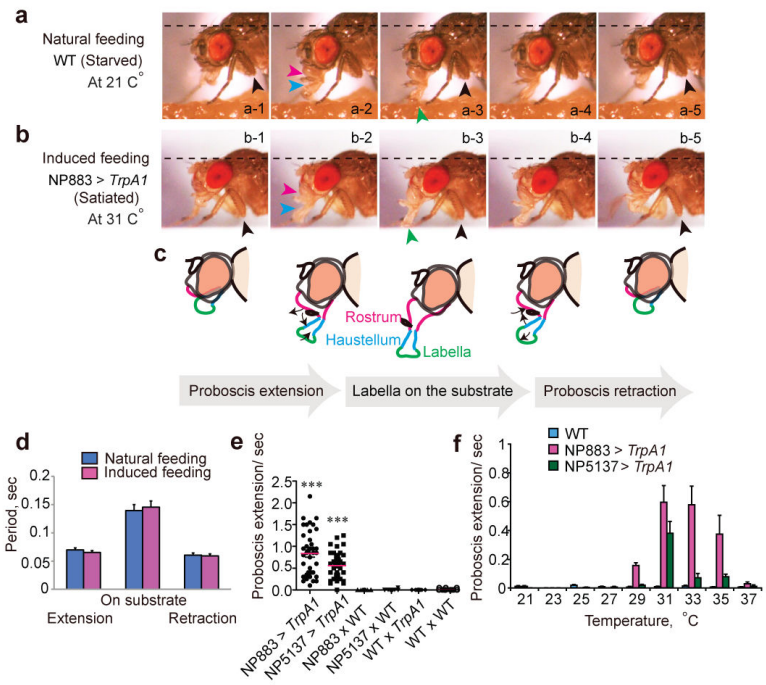

Figure 1. Thermo-genetic activation reproduced coordinated natural feeding behavior

a, Natural feeding behavior of a starved wildtype (WT) fly on normal food at 21°C. **b,** TrpA1-induced PE in a satiated NP883>*TrpA1* fly at 31°C. No food was present. **c,** Schematic drawings depict unfolding sequence of major segments of proboscis. **d,** Comparison of time taken for each step in proboscis extension in **c**. n= 22 for each genotype. **e**, PE rate of free-running, satiated flies observed singly in an arena without food at 31°C for each genotype. See Methods for description of the other line, NP5137, with a similar expression pattern to NP883 (Supplementary Fig. 8c). Magenta bars, mean values. Triple asterisks (***) denote P<0.001 (see Methods for statistics). n= 40 for each genotype. **f**, Temperature dependence of PE rate without food for free-running, satiated flies for each genotype. n= 40 for each genotype at each temperature. Error bars in all figures are SEM.

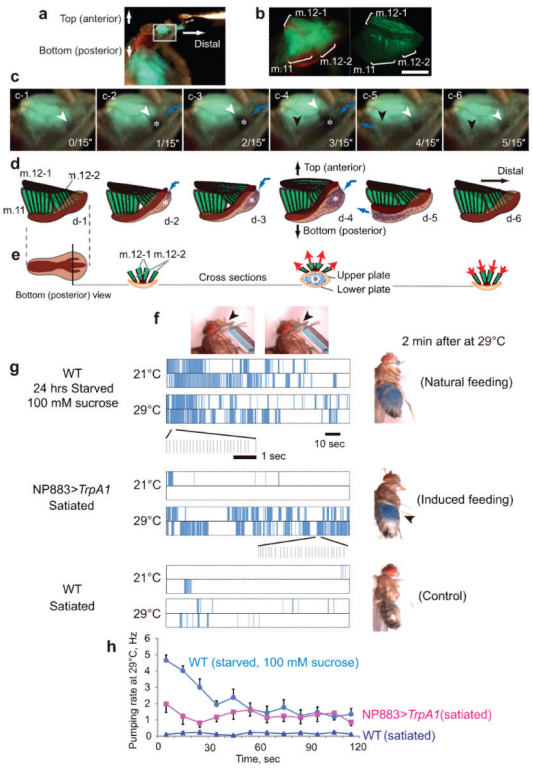

Figure 2. Thermo-genetically induced food ingestion through the pharyngeal pump

a-e, Mechanism of pharyngeal pump for normal ingestion in a WT fly. A fly starved for 24 hours was fed an aqueous 100 mM sucrose solution with blue dye. **a,** A side view. Muscles are highlighted with Myosin heavy chain (Mhc)-GFP. Area in white box is magnified in **c**. **b**, Micrographs (left, dissection microscope; right, confocal microscope) to illustrate muscle structure. Each of three muscle fiber groups, m.11, m.12-1, and m.12-2, consists of several muscle fibers, forming the pharyngeal pump. m.12-1 was described previously as 12[12], while m.12-2 was identified in this study with the help of Mhc-GFP. The scale bar, 100 μm. **c,** Still images at 21°C (Supplementary Video 3). White arrowheads, edge of m.12-1. Black arrowheads, edge of m.11. Blue arrows, flow of ingested material. Asterisks, the main lumen enlarged (also in **d**, **e**). **d, e,** Schematic diagram for muscles movement. The two sclerotized plates are depicted as light brown, whereas the apodeme, which protrudes from the upper plate and is attached to the muscles, is depicted as dark brown. **f,** Visualization of ingestion with blue dye in the space under m.12-1 and m.12-2 (arrowheads) for counting a single pulse in **g**. Left, closed state without dye; right, open state with dye. The proboscis of the fly was allowed to move freely as in its natural state. **g,** Representative raster plots (two for each condition) to show pumping events during a 2 minute period at 21°C and 29°C. Right, representative flies for each 29°C groups after 2 minutes. Arrowhead, belly with sugarless dye without starvation. **h,** Pumping rates plotted at every 10 sec in 29°C groups in **g.** n=11 (WT, sucrose), 11 (NP883>*TrpA1*), 18 (WT, control). Error bars, SEM.

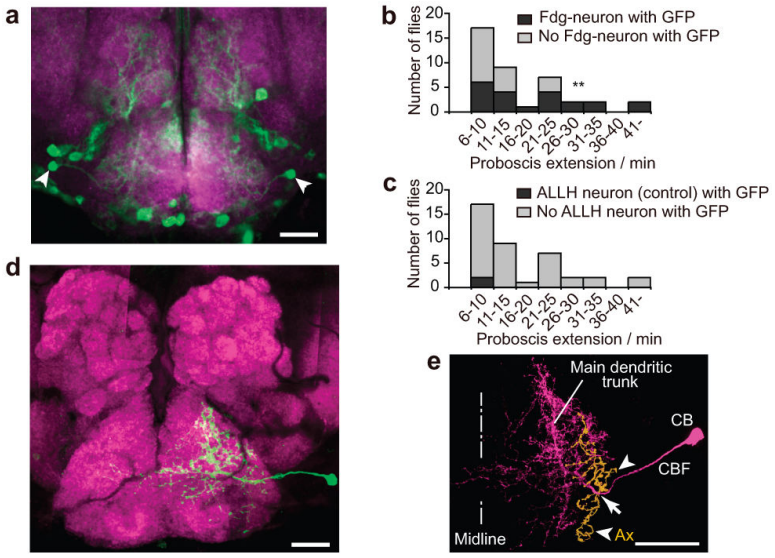

Figure 3. Identification of the Feeding (Fdg)-neuron

a, Full expression pattern of NP883 in the SEG as a confocal section, which covers both Fdg-neurons (Arrowheads). **b, c,** A histogram of PE rate in 40 PE-positive (PE > 5 times/min) flies, with GFP detected in Fdg-neuron (**b**) or ALLH (**c**) filled in black. Double asterisks, P<0.01 by Mann-Whitney's U-test between "with GFP" and "no GFP". **d,** The, "Fdg (feeding)-neuron", stained with anti-GFP antibody (green). A confocal montage of the SEG (lower half) and antennal lobes (upper half), with the neuropil marker antibody, nc82, (magenta). **e,** Fdg-neuron with the presumptive axon digitally traced in deep yellow, based on synaptic marker analyses in Supplementary Fig. 12. Arrow indicates position where the axon posteriorly branches off from cell body fiber (CBF), then, the sub-branches travel dorsally and ventrally as axon terminals (Ax, arrowheads). CB, cell body. All scale bars in this figure, 30 μm.

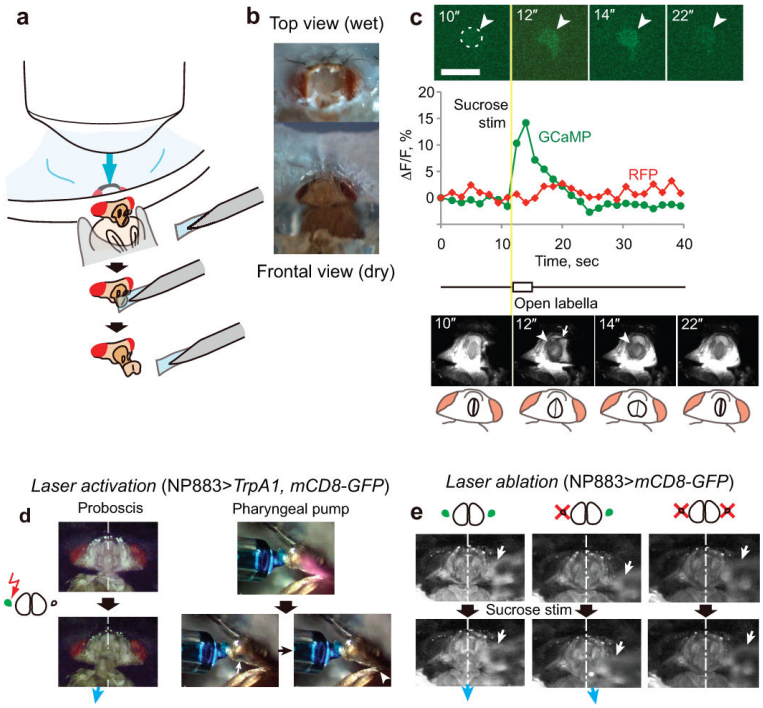

Figure 4. Functional analyses of Fdg-neuron

a, b, Experimental design with FLIES chamber[5] for experiments in this figure. **c,** Ca^{2+} imaging of Fdg-neuron when NP883>*GCaMP3.0*; *mCD8-RFP* flies were stimulated with 400 mM sucrose. Top, a representative GCaMP3.0 fluorescence at the cell body of Fdg-neuron (arrowheads) in a starved fly. Dashed circle, quantified area outlining an Fdg-neuron cell body. Scale bar, 10 μm. Middle, a time course of GCaMP3.0/RFP fluorescence as ratios to the initial fluorescence in a representative example. Bottom, labellar lobe opening (arrowheads) with other parts of proboscis immobilized. Arrow, sucrose wick for stimulation. Quantification and statistics are given in Supplementary Fig. 17. **d,** Laser activation of a single Fdg-neuron in a satiated fly. Left panels, Proboscis extension to the fly's right side in response to laser stimulation of the fly's right Fdg-neuron cell body to activate TrpA1 under a two-photon microscope. Right panels, Pump movement induced by laser activation of a single Fdg-neuron on either side. Dye solution was applied through a capillary tube as shown in Fig. 2f, to see ingestion through the pharyngeal pump (white arrow) and the esophagus (arrowhead) immediately after laser illumination. **e,** Laser ablation of a single Fdg-neuron. A cell body of a single Fdg-neuron was intensely illuminated under a two-photon microscope. Blue arrows, sucrose-induced PE directions before (left panels) and after (middle panels) ablation. The right panels, abolishment of sucrose-induced PE after ablation of both Fdg-neurons. Chain lines, fly's midline. White arrows, sucrose wick.